SECTION 2

The Cytoskeleton

CHAPTER 14

Correlated Light and Electron Microscopy of the Cytoskeleton

Sonja Auinger and J. Victor Small

Institute of Molecular Biotechnology
Dr Bohr-Gasse 3 1030
Vienna, Austria

METHODS IN CELL BIOLOGY, VOL. 88

0091-679X/08 $35.00
DOI: 10.1016/S0091-679X(08)00414-7

Abstract

The cytoskeleton of cultured cells can be most easily visualized in the electron microscope by simultaneous extraction and fixation with Triton–glutaraldehyde mixtures, followed by negative staining. Actin filaments are better preserved by stabilization with phalloidin, either during or after the primary fixation step. A technique is described for the combination of this procedure with live cell microscopy. Optimal conditions for light microscopy are achieved by culturing cells on coverslips coated with formvar film. For cell relocation a gold finder grid pattern is embossed on the film by evaporation through a tailor-made mask. After video microscopy and fixation, the film is floated from the coverslip and an electron microscope grid added to the film with the central hole of the grid over the region of interest. Accurate positioning is achieved under a dissecting microscope, using forceps mounted in a micromanipulator. Examples are shown of the changes in organization of actin filaments in the lamellipodia of migrating melanoma cells resulting from changes in protrusion rate. The technique is applicable to alternative processing procedures after fixation, including cryoelectron tomography.

I. Introduction

The turnover and rearrangement of actin filaments in cells is central to morphogenetic processes. Interactions of actin filaments with the cell membrane underlie the pushing and pulling that goes on, to change shape and to move and actin filaments provide the structural scaffolding for cell–cell and cell–substrate interactions, which likewise exert a primary influence on cell form. Actin filaments were first visualized by electron microscopy in plastic sections of muscle, and their helical substructure was deduced from negatively stained images of isolated native thin filaments or from actin polymerized *in vitro* (Huxley, 1969; Steinmetz *et al.*, 1997). When attention turned to visualizing actin arrangements in nonmuscle cells by electron microscopy, the results were disappointing. It soon became evident that plastic embedding procedures were unsuited to the visualization of actin filaments in arrays other than actin bundles stabilized by interactions with proteins such as tropomyosin and myosin (Goldman and Knipe, 1972) or other cross-linkers (Tilney *et al.*, 1980). Motile regions of cells, corresponding to ruffles or lamellipodia, were either devoid of structure (Abercrombie *et al.*, 1971), or appeared in thin sections as an amorphous, "fuzzy" matrix (Wessels *et al.*, 1973). Subsequent studies (reviewed in Small, 1988) showed that actin networks are distorted by procedures that include osmium tetroxide fixation and dehydration in organic solvents. Other procedures for visualizing the cytoskeleton were therefore adopted, each with their own advantages and pitfalls (see Small, 1988; Small *et al.*, 1999). To avoid plastic embedding, present methods are so far limited to cells thin enough to be taken directly into the electron microscope after appropriate processing. Current studies are thus restricted to cells in primary culture or to cell

lines. We will here focus on the technique of negative staining for contrasting, but will also discuss the applicability of the general approach to cryoelectron microscopy. Emphasis will be placed on correlating the movement of living cells in the light microscope with the organization of the actin cytoskeleton in the electron microscope. An alternative approach, described by Svitkina and coworkers (Svitkina and Borisy, 1999; Svitkina *et al.*, 1995, 2003), employs the critical point drying procedure and contrasting by rotary shadowing with platinum.

II. Materials and Methods

A. Materials

PBS
Chloroform
Formvar powder
MES, NaCl, EGTA, glucose, $MgCl_2$
Triton X-100
EM-grade glutaraldehyde
Phalloidin in MeOH (stock 1 mg/ml)
Alexa 488 or 568 Phalloidin 300U

B. Solutions

Formvar solution: 0.8–1% and 4% formvar in Chloroform; stir overnight in a closed container.

Cytoskeleton buffer (CB): 10 mM MES, 150 mM NaCl, 5 mM EGTA, 5 mM glucose, 5 mM $MgCl_2$; pH 6.1

Extraction solution: 0.25% glutaraldehyde (GA), 0.5% Triton, 1 μg/ml Phalloidin, 1:300 Alexa Phalloidin in CB; pH 6.5

Note: The ratios of glutaraldehyde and Triton can be adjusted to suit a given cell type.

Intermediate fixation solution: 2% GA, 1 μg/ml Phalloidin, 1:300 Alexa Phalloidin in CB; pH 7

Post-fixation solution: 2% GA, 10 μg/ml Phalloidin in CB; pH 7

Negative stain solutions:

4% sodium silicotungstate (SST)
2% SST
2% SST + 1% aurothioglucose
1% SST + 1% aurothioglucose

These solutions need to be pH adjusted (to around pH 7.5) and filtered (0.2 μm)! For pH adjustment it is important to avoid any intake of salts (use only NaOH) and to check pH every few days until it is stable.

III. Methods

A. Patterned Thin Films for Correlated Light Microscopy

To combine light microscopy with the electron microscopy, cells can be grown on filmed electron microscope grids and imaged live with the grid inverted in a growth chamber on the light microscope (Resch, 2006; Rinnerthaler *et al.*, 1991). The preparation is fixed at an appropriate time and processed for electron microscopy. By using a finder grid, the cell observed by light microscopy is readily located in the electron microscope. While this technique works well (Resch *et al.*, 2006), optimal resolution is difficult to achieve on the freely suspended film in the light microscope. We have therefore adopted a modification, originally introduced by Buckley and Porter (1967), that employs coverslips coated with formvar films. For the purpose of cell relocation, a finder grid pattern is coated onto the film. This method facilitates light microscopy under more suitable imaging conditions. The method can of course be used without a finder pattern, when identification of the same cell in the light and electron microscope is not required.

The procedure for substrate preparation is illustrated schematically in Fig. 1. A formvar film (FV) is cast on a glass slide and floated onto a water trough as usual (Steps 1–4, Fig. 1). Coverslips that fit in the incubation chamber of the light microscope are prepared beforehand: these are dipped and dried in a solution of 2.5% Triton X-100 (to ensure later release of the film) and then coated on their rim with a concentrated solution of formvar (4%), applied through a pipette tip (Step 5, Fig. 1). The latter step is necessary to facilitate later handling of the film. The coverslips are then added to the floating formvar film and retrieved with a piece of parafilm (Steps 6 and 7, Fig. 1). After drying, the coverslips are covered with copper grid masks and coated with gold in an evaporation unit (Step 8, Fig. 1).

The grid masks are custom made "negative grids" (Small, 1984) from Pyser (Edenbridge, UK) in which the grid bars are open and the squares closed (Fig. 2), so that a finder grid pattern is deposited on the film. The amount of gold deposited through the mask should be sufficient that the pattern is easily visible under a dissecting microscope. The masks are made from thin copper foil, have a total diameter of 15 mm and contain 9, separately numbered grid patterns to allow more choice in the selection of suitable cells (Fig. 2). The masks are glued to steel washers to facilitate handling and to keep them flat and can be reused many times.

The coverslip-film combination is sterilized under UV, coated with connective tissue components as required and cells plated onto the film. The cells are transfected with probes of interest expressing EGFP and RFP tags (Shaner *et al.*, 2004) 1–2days before plating.

B. Live Cell Microscopy and Fixation

Imaging of cells can be performed in different modes (wide field, confocal, or TIRF), depending on the experimental requirements. We routinely use wide field imaging on a Zeiss Axiovert 200 inverted microscope equipped with a rear

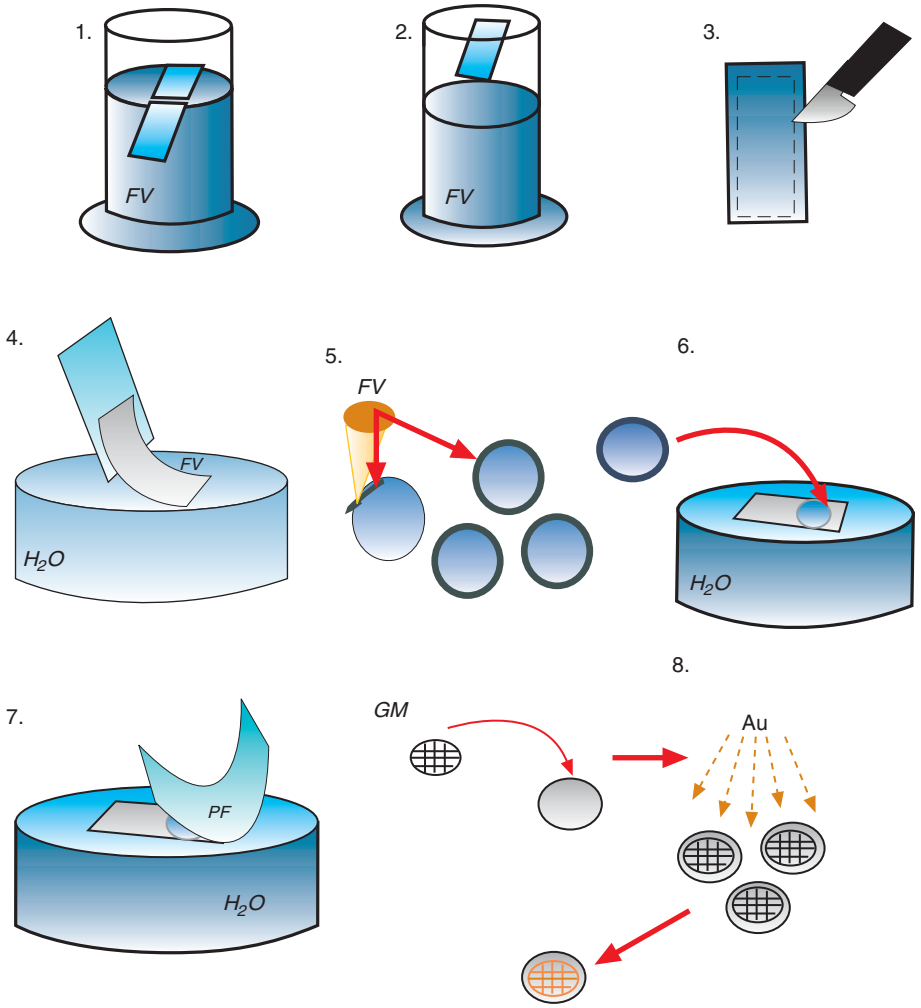

Fig. 1 Preparation of the support films for correlated light and electron microscopy. A formvar film is cast on a cleaned glass slide by dipping into a formvar solution (FV) in a measuring cylinder and drying in the cylinder above the liquid surface (Steps 1 and 2). After scoring on the edge (Step 3), the film is floated onto a water surface (Step 4). Coverslips required for light microscopy are precoated on the edge with a thick rim of formvar (4%) through a pipette tip (Step 5). The coverslips are added to the floating film and retrieved with a piece of parafilm, PF (Step 7). After drying, the coverslips are individually covered with a grid mask (GM), transferred to a vacuum evaporator and coated with a thin layer of gold (Step 8).

illuminated, cooled CCD camera (Micromax, Roper Scientific), and filter wheel and shutter systems for alternating phase and fluorescence microscopy. Transmitted (phase contrast) and incident illumination (fluorescence) is provided by halogen or mercury lamps (with intensity control), with times between subsequent

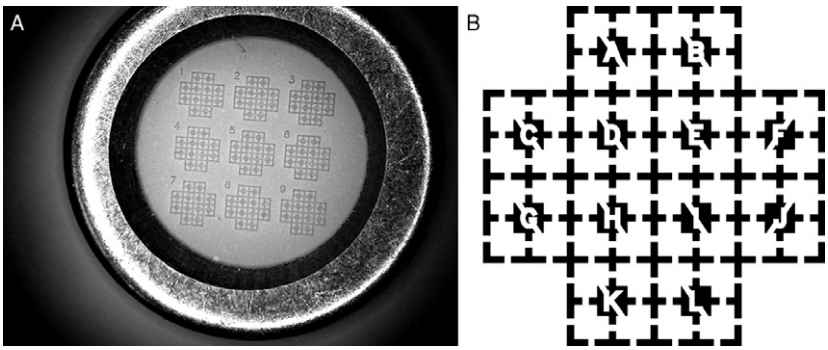

Fig. 2 The negative grid mask. (A) The copper film mask, containing nine finder patterns, mounted on a washer for easy handling. The outside diameter of the mask is 15 mm. (B) The finder pattern in which the black areas correspond to the open regions in the copper film.

frames ranging from 2 to 20 s. Imaging is performed with an oil immersion 100×, NA1.4 objective lens.

Two types of chambers are employed for imaging: an open chamber from Harvard Instruments (Nr, 64 0232) mounted on a heating platform and a home-made, flow through chamber that fits on the same platform. Similar results have been obtained with either chamber, and for simplicity, we will confine discussion to the open system that is commercially available. In the absence of a CO_2 cabinet around the microscope, we use a CO_2-independent culture medium and limit observation to normally less than 1 h. At a chosen time during imaging, the cell of interest is arrested by exchange of the growth medium for the extraction/fixation mixture, containing glutaraldehyde (0.25%), Triton (0.5%), and optionally, 1 μg/ml phalloidin in a cytoskeleton buffer (CB). After around 1 min, the fixation/extraction mix is exchanged for the intermediate fixation solution, including optionally fluorescent phalloidin, to record an actin image of the fixed cell while still on the microscope. The coverslip is then removed from the chamber and transferred to the post-fixation solution, which also includes phalloidin. Post-fixation is performed for at least 30 min at RT and is typically continued overnight at 4 °C. Cells can be kept in this solution for several days at 4 °C before further processing.

C. Cell Relocation and Negative Staining

The next step involves removal of the film from the coverslip, location of the grid square carrying the imaged cell and the application of an EM grid onto the film with the cell in the centre of the grid. This is achieved by following the steps depicted in Figs. 3 and 4.

The coverslip is placed, film side up in a 9-cm Petri dish containing CB. Using forceps, the film is carefully detached from the edge of the coverslip where it is supported by the thick formvar rim. With two pairs of forceps the film is then inverted and brought to the buffer surface so that it spreads out by surface tension,

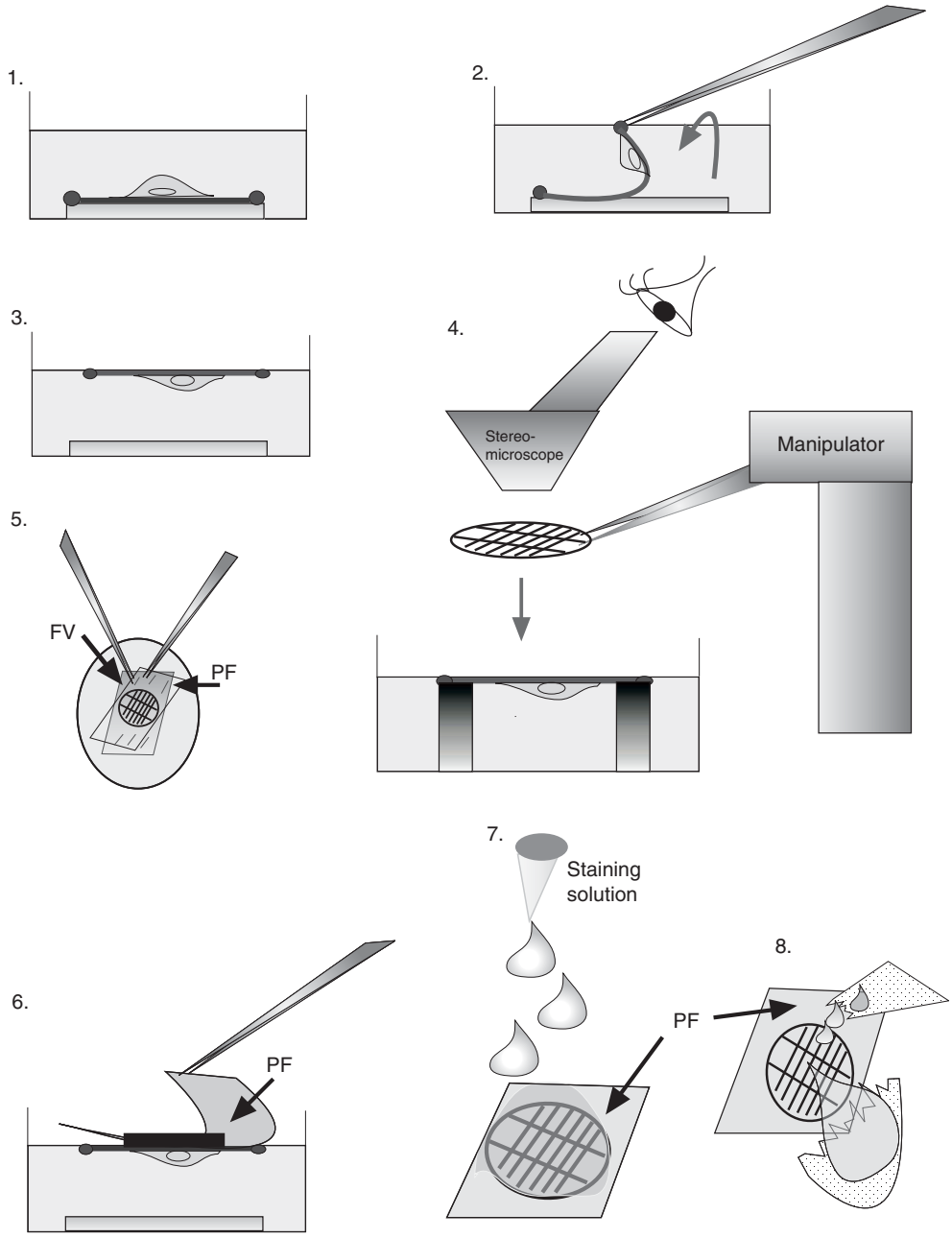

Fig. 3 Film retrieval and negative staining. With the coverslip immersed in CB in a Petri dish (Step 1), the film is loosed on the edges and flipped onto the buffer surface, with the cells down (Steps 2 and 3). Under a dissecting microscope, the film is maneuvered onto a ring and the grid placed on the film using forceps mounted in a micromanipulator (Step 4). Parafilm is layed over the floating grid and the parafilm and formvar film pressed together at the periphery with forceps (Step 5). The parafilm-grid combination is then removed, rinsed with several drops of stain and blotted on the edge with filter paper (Steps 6–8).

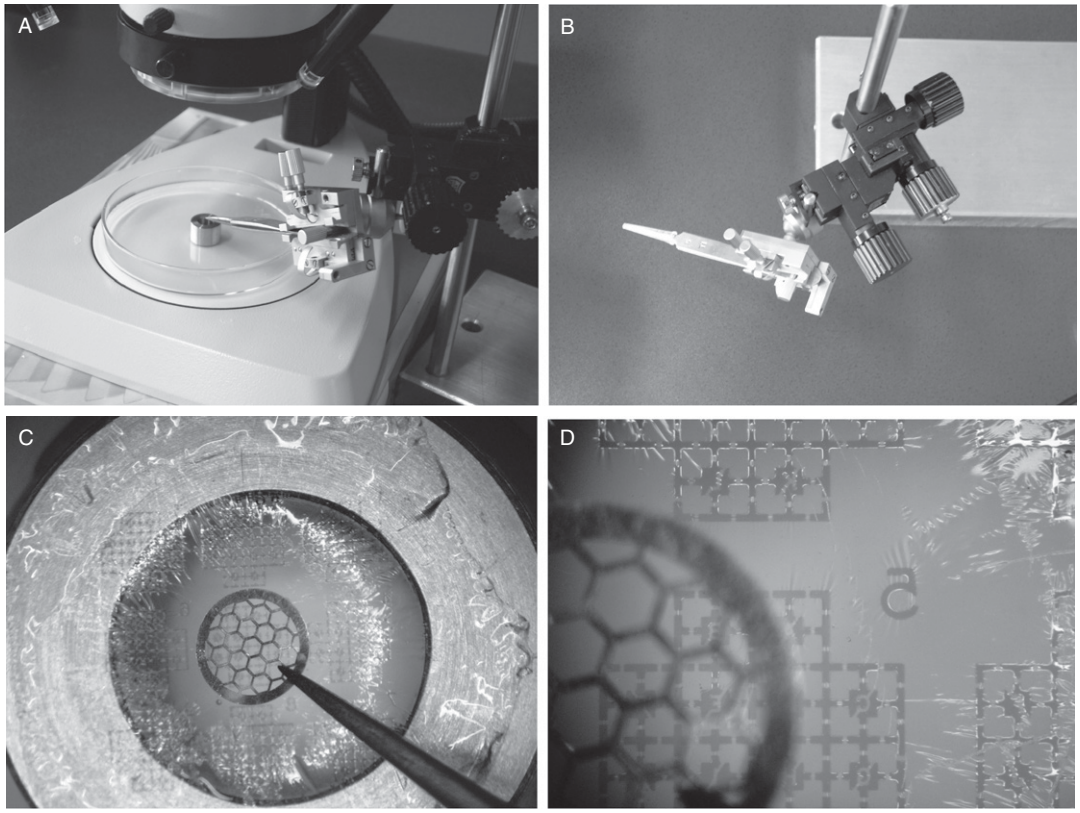

Fig. 4 Maneuvering the grid onto the film. (A) Overview of the mounting set-up. (B) Forceps in the modified dual pipette holder, mounted on the micromanipulator. (C) Application of the grid with the film immobilized on the support ring. (D) Close-up view of the 50 mesh hexagonal grid over the finder grid pattern on the film.

with the cells facing down (Steps 2 and 3; Fig. 3). Next, the film is immobilized on a stainless steel ring platform (height, 1 cm, inner and outer diameters 8 and 15 mm, respectively; Fig. 4A and C) by floating it over the ring and removing enough liquid from the dish to capture the film, with the grid pattern centered (Fig. 4D). Under a dissecting microscope, a 50 mesh hexagonal copper grid is placed onto the film so that the cell of interest lies in the central hole. This is achieved using forceps in a micromanipulator to hold the grid, with an arrangement that allows gentle release of the grid onto the film. For this operation, we use a modified dual pipette holder from Leica to hold the forceps, fixed on a manual micromanipulator from Narashiga (Fig. 4B).

The grid is retrieved and negatively stained as depicted in Steps 5–8 in Fig. 3. With the grid attached, the film is floated off the platform and covered with a piece of parafilm not much larger than the film. Forceps are used to press the floating

film to the parafilm surface (Step 5) so that it remains attached in the next step. The parafilm–film combination is removed from the dish with forceps, rinsed on the cell side with several drops of negative staining solution and blotted on the sides with the torn edge of a filter paper (Steps 6–8; Fig. 3). Care should be taken that no macroscopic drops remain on the grid. After drying, the grid can be observed in the microscope. To prevent recrystallization of the stain by uptake of moisture from the atmosphere, grids should be stored in an exicator, but are preferably observed immediately.

Neutral negative stains have been found to be most suitable for cytoskeleton preparations (see also Hoglund *et al.*, 1980). We have used sodium silicotungstate, phosphotungstic acid, and mixtures of sodium silicotungstate with aurothioglucose or trehalose. The concentrations tried range from 1 to 4%, with the pH adjusted between 7 and 8. Acidic uranyl acetate gives high contrast, but the actin filaments are more distorted, suggestive of undue collapse of actin networks during drying Small, J. V., and Celis, J. E. (1978). This contrasts with the results obtained with uranyl acetate for synthetic actin filaments stabilized on a support film, as evidenced from the wealth of literature on actin filament ultrastructure (e.g., Steinmetz *et al.*, 1997). Some three dimensionality of lamellipodia networks is preserved in sodium silicotungstate, as can be illustrated with stereopairs (Small, 1981, 1988) and actin filament substructure is readily visualized in bundles of actin, in filopodia (Small, 1981). Neutral uranyl acetate, buffered with EDTA, can also give good contrast (Resch, private communication), but has not been used enough on cytoskeletons to warrant discussion of its potential here. Suffice it to say that there is room for more experimentation with new mixtures of heavy metal stains for contrasting cytoskeletons.

D. A Note on the Fixation Procedure

The fixation protocol described earlier, comprising a mixture of glutaraldehyde, Triton, and phalloidin (optional), has evolved from original efforts to preserve cell morphology by rapid fixation and at the same time extract cells sufficiently to make the cytoskeleton visible (see Small, 1988; Small *et al.*, 1999). The most suitable ratio of glutaraldehyde to Triton will depend on cell type and should be first assessed in control experiments. Phalloidin has a dual function: as a fluorescent label to control actin preservation in the fluorescence microscope and as a stabilizer of actin filaments. Without phalloidin, actin filaments in negatively stained cytoskeleton networks are often distorted, presumably because they are more susceptible to drying effects than filaments directly attached to the supporting film. Most of our earlier studies employed phalloidin after fixation. However, for correlated live cell microscopy and EM, we have found it advantageous to include phalloidin in the primary fixative. Since the basic structural details are the same, whether phalloidin is added during or after fixation, it appears that the time of cell arrest by the fixative mixture (a fraction of a second) is too short for phalloidin to modify the endogenous filament pool.

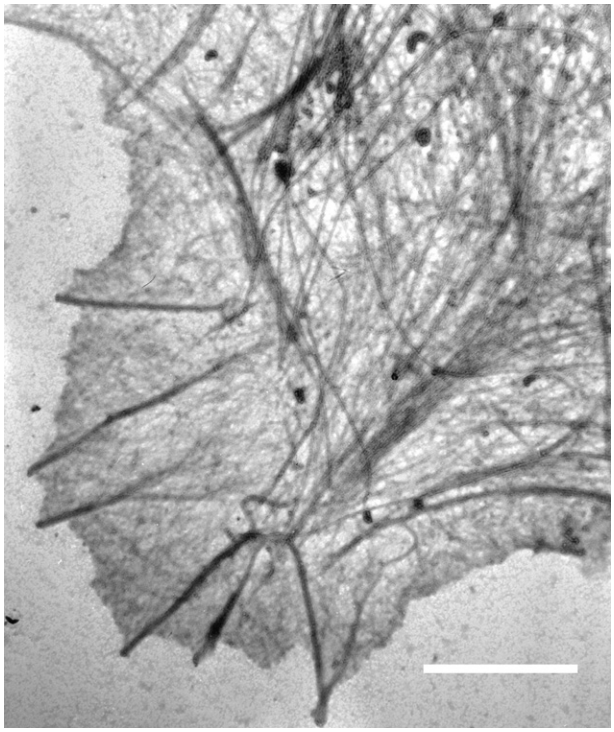

Fig. 5 Low magnification view of the peripheral region of a fish fibroblast cytoskeleton (initial fixation: 0.5%Triton; 0.25%glutaraldehyde), stained with 2% sodium silicotungstate. Bar, 2 μm.

IV. Results and Discussion

A. Structural Features in Cytoskeleton Preparations

Figures 5 and 6 show some general features of negatively stained cytoskeletons prepared by simultaneous extraction and fixation with Triton–glutaraldehyde mixtures. At low magnification, cells should display a continuous, nonfragmented cell edge and a smooth appearance of lamellipodia. The appearance of holes is diagnostic of poor preservation or poor staining. The spreading cell edges show actin networks and actin bundles (filopodia), with all transition stages in between (Fig. 6A; Small, 1988; Small *et al.*, 1982). Behind the lamellipodium, in the so-called lamella zone, the three filament systems of the cytoskeleton can be distinguished (Fig. 6B).

B. Correlated Light and Electron Microscopy

We give two examples here of correlated light microscopy and electron microscopy of motile B16 melanoma cells. In both cases, the cells were treated with aluminum fluoride, which leads to the activation of Rac and to continuous

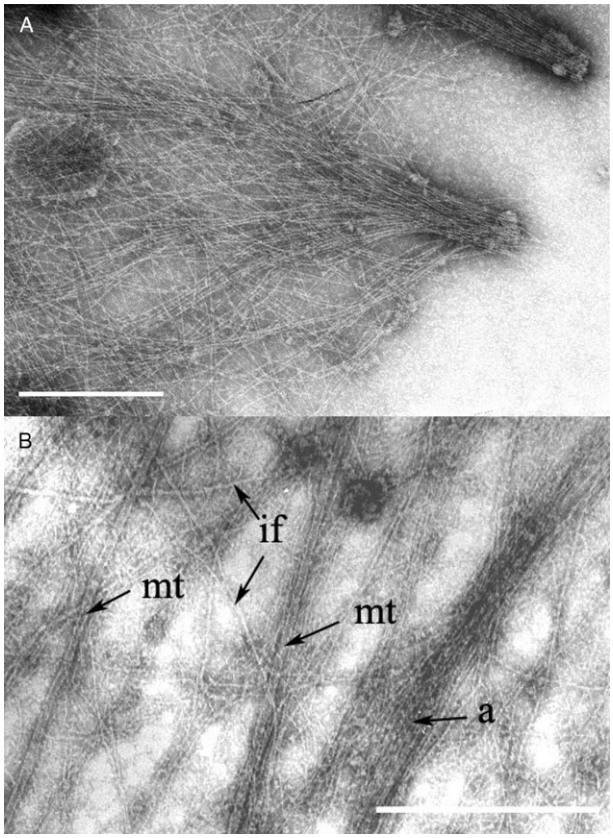

Fig. 6 (A) Details of a cell edge, in the region of a transition between the lamellipodium network and a filopodium. (B) A lamella region showing the three filaments of the cytoskeleton: actin, a; intermediate filaments, if and microtubules, mt. Bars, 0.5 μm.

protrusive activity over a period of around 30–60 min. In the first example (Fig. 7), the cell was fixed at an early stage of stimulation, when protrusion over the whole cell front was continuous at about 1 μm/min. The cell was transfected with GFP-VASP, which localizes to adhesion structures and to the tips of protruding lamellipodia (Rottner *et al.*, 1999). The figure shows the first and last frames of the video of the cell in the GFP channel on the fluorescence microscope, up to the fixation step (Fig. 7A) and the overview of the cell in the EM (Fig. 7B). An overlay of the EM image with the last frame of the video (not shown) confirmed that the cell was rapidly arrested by the fixation step. The region boxed in the overview is depicted at high magnification in Fig. 7C and shows a distinct diagonal network of actin filaments in the protruding lamellipodium.

In the second example (Fig. 8), the cell was fixed at a later stage of aluminum fluoride stimulation, when the protrusion rate was decreasing to different degrees

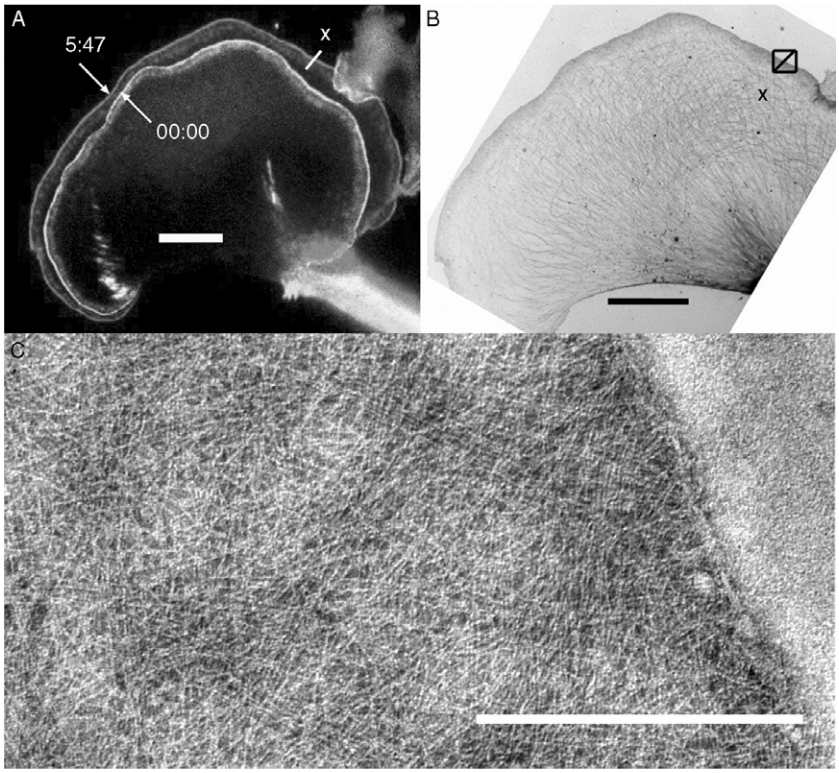

Fig. 7 Correlated light and electron microscopy of a B16 melanoma cell tagged with VASP-GFP. A. First and last video frames (5 s between frames) of the living cell, taken at the times indicated. Cell was fixed immediately after the final frame at 5 min 47 s. In the region indicated by the white line, the cell front was advancing continuously in the final 30 s at 1 μm/min. (B) EM overview; boxed region corresponds to position shown in (A) and to the close up in (C). (C) Actin filament organization in the region indicated in (A) and (B). Note more or less regular diagonal network of filaments. Bars: A and B, 10 μm; C, 0.5 μm.

along the cell edge. Again, the cell was transfected with GFP-VASP, in this case resulting in a lower expression as compared to Fig. 7. Figure 8A and B correspond to the first and last frames of the video and C to the EM overview of the cell, fixed immediately after the last frame. The regions marked "x" and "y" in the final video frame correspond to sites on the cell edge that were moving slowly, 0.8 μ/min (x) or that were stationary (y) during the final 30 s of the video. The same positions are marked on the EM overview. Note that a decrease in protrusion rate is associated with a less organized actin network (Fig. 9A) than seen in Fig. 7C. And the arrest of protrusion is associated with the development of actin arrays parallel to the cell edge (Fig. 9B), through a rearrangement of filaments in the lamellipodium (see also Rinnerthaler *et al.*, 1991; Small *et al.*, 1998).

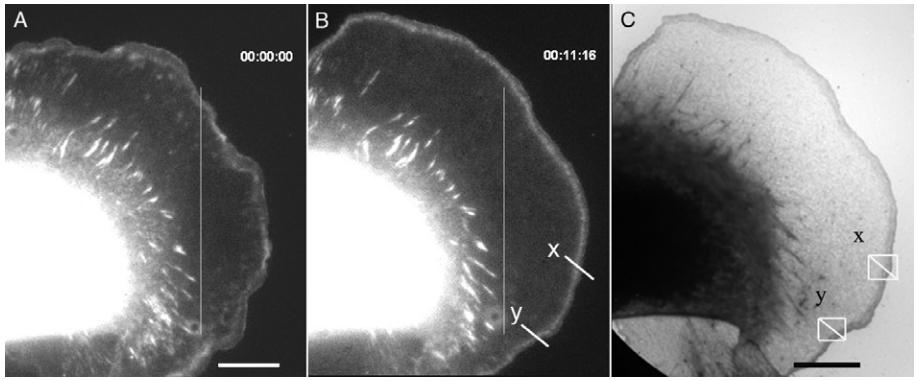

Fig. 8 (A and B) The first (0.0 min) and last video frame (11 min 16 s) of a B16 melanoma cell transfected with VASP-GFP. The vertical white line marks a reference position in the cell. (C) Overview of the cell in the EM. The positions marked "x" and "y" correspond to sites where the cell edge was stationary during the final 30 s (y) and moving forward at 0.8 μm/min(x). The same positions are marked on (C) and shown at higher magnification in Fig. 9. Bars, 10 μm.

C. Evaluation of the Technique

With the method described, the success rate of cells that make it from the light microscope to the EM is in the range of 50%. The yield of good cells with clear filament contrast is a little lower, owing to some uncontrolled variability in the depth of the negative stain. Actin filaments, intermediate filaments and microtubules are clearly resolved. In particular the rearrangements of actin at the cell front, associated with motility and adhesion are most accessible by this technique. Some variability in staining does however occur, leading to cells that are too weakly or too strongly contrasted. Whatever method may be employed, it is important to have light microscope controls of the extraction/fixation process to ensure that it faithfully arrests the cell without visibly changing morphology. The use of GFP tagged proteins is obviously advantageous as it opens up the possibility of controlling more structural parameters. Using cells tagged with actin-GFP, we have monitored the fixation process by live cell microscopy and shown that the Triton–glutaraldehyde mixtures described here preserve the gradient of actin density in the lamellipodium (Koestler *et al.*, 2008).

In an alternative approach for correlated light and electron microscopy, Svitkina *et al.* (1995) have developed a procedure based on processing of cells for critical point drying and contrasting by metal shadowing. The advantage of this technique is that the cells can be grown on glass coverslips and processed on the coverslips through to the metal coating stage. The replica is then floated off and the picked up on a formvar film under a dissecting microscope. This technique has been used to great advantage in studies of the cytoskeleton (Biyasheva *et al.*, 2004; Svitkina and Borisy, 1999; Svitkina *et al.*, 2003). One drawback of this approach is

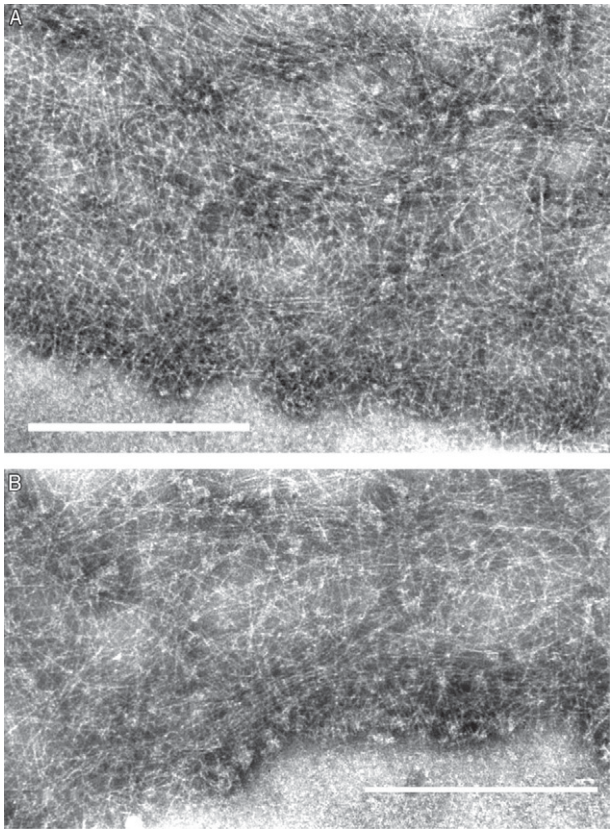

Fig. 9 (A) and (B) correspond respectively to the slowly advancing region "x" and the stationary region "y" in Fig. 8B and to the boxed regions in Fig. 8C. See text for details. Bars, 0.5 μm.

the requirement for multiple processing steps after fixation, which can potentially introduce artifacts (Resch *et al.*, 2002a).

The general technique of live cell imaging on support films described here can in principle be adapted for other procedures. Cytoskeletons prepared by extraction with detergent alone can be "dissected" to remove specific components before fixation to reveal other details, for example by the use of actin depolymerising proteins (Small *et al.*, 1982; Svitkina *et al.*, 1996; Verkhovsky *et al.*, 1995) and inhibitors. Likewise, alternative processing and imaging modes can be employed, including critical point drying (Svitkina *et al.*, 1995) and cryo-EM (Resch *et al.*, 2002b). In view of the new possibilities opened by cryo-EM tomography (Medalia *et al.*, 2002), cytoskeleton preparations for which correlated live cell imaging was performed offer interesting potential for correlating structure and function. The latter technique, combined with new methods for tagging

proteins for recognition in the EM, promises to open important new avenues in cytoskeleton research.

V. Summary

The technique described here is applicable to the thin regions of cultured cells, which are well preserved after embedding in negative stain. Some degree of three-dimensionality is inevitably lost during drying, particularly in lamella regions behind the lamellipodium. The present methods have been used to advantage to relate the organization and filament density in lamellipodia to protrusion speed (Koestler *et al.*, 2008). Further advances are to be expected from the development of new methods for high-resolution protein localization and the application of cryoelectron tomography to gain three-dimensional information of filament arrangements and interconnections.

Acknowledgements

We thank Guenter Resch for discussion and assistance with electron microscopy

References

Abercrombie, M., Heaysman, J. E., and Pegrum, S. M. (1971). The locomotion of fibroblasts in culture. IV. Electron microscopy of the leading lamella. *Exp. Cell Res.* **67,** 359–367.

Biyasheva, A., Svitkina, T., Kunda, P., Baum, B., and Borisy, G. (2004). Cascade pathway of filopodia formation downstream of SCAR. *J. Cell Sci.* **117,** 837–848.

Buckley, I. K., and Porter, K. R. (1967). Cytoplasmic fibrils in living cultured cells. A light and electron microscope study. *Protoplasma* **64,** 349–380.

Goldman, R. D., and Knipe, D. M. (1972). Functions of cytoplasmic fibers in non-muscle cell motility. *In* "Cold Spring Harbor Symposium on Quantitative Biology." Vol. XXXVII, Cold Spring Harbor, pp. 523–534.

Hoglund, A. S., Karlsson, R., Arro, E., Fredriksson, B. A., and Lindberg, U. (1980). Visualization of the peripheral weave of microfilaments in glia cells. *J. Muscle Res. Cell Motil.* **1,** 127–146.

Huxley, H. E. (1969). The mechanism of muscular contraction. *Science* **164,** 1356–1365.

Koestler, S. A., Auinger, S., Vinzenz, M., Rottner, K., and Small, J. V. (2008). Differentially oriented populations of actin filaments generated in lamellipodia collaborate in pushing and pausing at the cell front. *Nature Cell Biol.***10,** 306–313.

Medalia, O., Weber, I., Frangakis, A. S., Nicastro, D., Gerisch, G., and Baumeister, W. (2002). Macromolecular architecture in eukaryotic cells visualized by cryoelectron tomography. *Science* **298,** 1209–1213.

Resch, G. P., Goldie, K. N., Hoenger, A., and Small, J. V. (2002a). Pure F-actin networks are distorted and branched by steps in the critical-point drying method. *J. Struct. Biol.* **137,** 305–312.

Resch, G. P., Goldie, K. N., Krebs, A., Hoenger, A., and Small, J. V. (2002b). Visualisation of the actin cytoskeleton by cryo-electron microscopy. *J. Cell Sci.* **115,** 1877–1882.

Resch, G. P., Small, J. V., and Goldie, K. N. (2006). Electron microscopy of the cytoskeleton: negative staining, cryo-EM and correlation with light microscopy. *In* "Cell Biology: A Laboratory Handbook III" (J. E. Celis, ed.), Vol. 3, pp. 267–275. Academic Press.

Rinnerthaler, G., Herzog, M., Klappacher, M., Kunka, H., and Small, J. V. (1991). Leading edge movement and ultrastructure in mouse macrophages. *J. Struct. Biol.* **106,** 1–16.

Rottner, K., Behrendt, B., Small, J. V., and Wehland, J. (1999). VASP dynamics during lamellipodia protrusion. *Nat. Cell Biol.* **1,** 321–322.

Shaner, N. C., Campbell, R. E., Steinbach, P. A., Giepmans, B. N., Palmer, A. E., and Tsien, R. Y. (2004). Improved monomeric red, orange and yellow fluorescent proteins derived from *Discosoma* sp. red fluorescent protein. *Nat. Biotechnol.* **22,** 1567–1572.

Small, J., Rottner, K., Hahne, P., and Anderson, K. I. (1999). Visualising the actin cytoskeleton. *Microsc. Res. Tech.* **47,** 3–17.

Small, J. V., and Celis, J. E. (1978). Filament arrangements in negatively stained cultured cells: The organization of actin. *Eur. J. Cell Biol.* **16,** 308–325.

Small, J. V. (1981). Organization of actin in the leading edge of cultured cells: Influence of osmium tetroxide and dehydration on the ultrastructure of actin meshworks. *J. Cell Biol.* **91,** 695–705.

Small, J. V. (1984). Simple procedures for the transfer of grid images onto glass coverslips for the rapid relocation of cultured cells. *J. Microsc* **137,** 171–175.

Small, J. V. (1988). The actin cytoskeleton. *Electron. Microsc. Rev.* **1,** 155–174.

Small, J. V., Rinnerthaler, G., and Hinssen, H. (1982). Organization of actin meshworks in cultured cells: the leading edge. *Cold Spring Harb. Symp. Quant. Biol.* **46**(Pt. 2), 599–611.

Small, J. V., Rottner, K., Kaverina, I., and Anderson, K. I. (1998). Assembling an actin cytoskeleton for cell attachment and movement. *Biochim. Biophys. Acta* **1404,** 271–281.

Steinmetz, M. O., Stoffler, D., Hoenger, A., Bremer, A., and Aebi, U. (1997). Actin: From cell biology to atomic detail. *J. Struct. Biol.* **119,** 295–320.

Svitkina, T. M., and Borisy, G. G. (1999). Arp2/3 complex and actin depolymerizing factor/cofilin in dendritic organization and treadmilling of actin filament array in lamellipodia. *J. Cell. Biol.* **145,** 1009–1026.

Svitkina, T. M., Bulanova, E. A., Chaga, O. Y., Vignjevic, D. M., Kojima, S., Vasiliev, J. M., and Borisy, G. G. (2003). Mechanism of filopodia initiation by reorganization of a dendritic network. *J. Cell. Biol.* **160,** 409–421.

Svitkina, T. M., Verkhovsky, A. B., and Borisy, G. G. (1995). Improved procedures for electron microscopic visualization of the cytoskeleton of cultured cells. *J. Struct. Biol.* **115,** 290–303.

Svitkina, T. M., Verkhovsky, A. B., and Borisy, G. G. (1996). Plectin sidearms mediate interaction of intermediate filaments with microtubules and other components of the cytoskeleton. *J. Cell. Biol.* **135,** 991–1007.

Tilney, L. G., Derosier, D. J., and Mulroy, M. J. (1980). The organization of actin filaments in the stereocilia of cochlear hair cells. *J. Cell. Biol.* **86,** 244–259.

Verkhovsky, A. B., Svitkina, T. M., and Borisy, G. G. (1995). Myosin II filament assemblies in the active lamella of fibroblasts: Their morphogenesis and role in the formation of actin filament bundles. *J. Cell. Biol.* **131,** 989–1002.

Wessels, N. K., Spooner, B. S., and Luduena, M. A. (1973). Surface movements, microfilaments and locomotion. *In* "Ciba Found. Symposium on Locomotion of Tissue Cells," Vol. 14, pp. 53–77. Elsevier, Amsterdam.